Luminaire Detection through Brightness Enhanced Mask R-CNN in Tunnel Environment

Bintao Xu[1], Lirui Liu[3, 4], Xiaoqiong Qin[1, 2], Linfu Xie[3, 4]

[1] State Key Laboratory of Intelligent Geotechnics and Tunnelling, Shenzhen University, Shenzhen 518060, China

[2] Shenzhen Technology Institute of Urban Public Safety, and Key Laboratory of Urban Safety Risk Monitoring and Early Warning, Ministry of Emergency Management, Shenzhen 518060, China

[3] State Key Laboratory of Subtropical Building and Urban Science, Shenzhen University, Shenzhen 518060, China

[4] Research Institute for Smart Cities, School of Architecture and Urban Planning, Shenzhen University, Shenzhen 518060, China

xbt593169742@163.com, 2410114001@mails.szu.edu.cn, (xqqin, linfuxie)@szu.edu.cn

Keywords: Mask R-CNN, Object Detection, Tunnel Luminaires, Object Brightness Enhancement.

Abstract

Rapid luminaire detection enables effective remote monitoring and management, thereby facilitating intelligent tunnel lighting maintenance. Despite its powerful object detection capabilities, deep learning methodologies encounter challenges in tunnel luminaire detection due to the complex environment and unfavorable lighting conditions. To overcome these issues, this paper proposes an improved tunnel luminaire detection solution by enhancing the Mask R-CNN using brightness balancing. Leveraging tunnel gray-scale images and the Mask R-CNN object detection framework, a feature fusion network based on ResNet-FPN, trained via transfer learning, which enhances performance in detecting object luminaires. Furthermore, considering the differences in luminaire brightness and their backgrounds, an object brightness enhancement method based on Kapur's Entropy Method is introduced to effectively reducing missed detections and false positives, thereby improving the detection rate of luminaires. To evaluate the performance of the proposed approach, real datasets of tunnel environment are used. Experimental results revealed that the proposed approach achieved precision, recall, an F1-score and AP50 of 94.9%, 82.3%, 0.881 and 0.776, respectively, which improved of 4.3%, 4.4%, 0.044, and 0.151, respectively, compared to the original model, thus, could be applied to the 3D model construction and intelligent management of tunnels.

1. INTRODUCTION

Tunnel lighting is crucial for ensuring safety and efficiency in modern urban transportation systems, directly impacting traffic flow and daily convenience (Hou et al. 2018). Traditional tunnel lighting systems, which often rely on manual inspection, face challenges such as low management efficiency, significant energy waste, and high maintenance costs. To address these issues, researchers have proposed intelligent management and automated control solutions for tunnel lighting, with luminaire object detection and localization technology being crucial to achieving intelligent tunnel lighting management.

Current research on extracting objects for tunnel luminaires remains relatively scarce. Early studies can be categorized into two main approaches: point cloud-based methods and image-based methods. Point cloud-based methods rely on light detection and ranging (LiDAR) technology to obtain three-dimensional point cloud data, filtering the data based on height and color intensity features to locate tunnel luminaires (Puente et al. 2014). Image-based methods use traditional image processing techniques to process data from vehicle-mounted cameras, thereby identifying tunnel luminaires (Lu et al. 2015; Xin et al. 2021). While LiDAR technology is known for its high-precision three-dimensional data capture capabilities, it is limited by high costs, complex data processing requirements, and susceptibility to interference in complex environments. In contrast, image-based methods offer cost-effectiveness, ease of data acquisition, and effortless system integration despite their dependency on image quality and sensitivity to lighting conditions. With the rapid development of deep learning technologies, especially the widespread application of Convolutional Neural Networks (CNNs), image-based processing methods have demonstrated excellent performance in feature extraction and object detection, partially overcoming the limitations of traditional methods (Yang et al. 2021). In tunnel luminaire detection, deep-learning methods like YOLOv5 (Dai et al. 2022) and segmentation models DeepLab/U-Net (Alidoost et al. 2023) have been applied. However, challenges persist due to the need for well-annotated datasets and complex tunnel lighting conditions that affect detection success rates.

The detection of tunnel luminaires has seen advancements, but improving accuracy in low-light tunnel environments remains challenging due to low illumination and noise in the images (Yang et al. 2020). Low-light image enhancement methods are mainly divided into traditional algorithms and deep learning algorithms. Traditional algorithms, such as histogram enhancement and Retinex methods, adjust pixel distribution or decompose images into illumination and reflection components to enhance brightness and contrast (Pizer et al. 1987; Jobson et al. 1997). However, these methods rely on manually designed constraints, limiting their adaptability and generalization. Deep learning algorithms have shown significant progress in recent years, with supervised, unsupervised, and zero-shot learning strategies. Supervised learning methods, such as Retinex-Net, require paired low-light/normal-light images for training and offer good enhancement effects but face difficulties in obtaining paired data (Wei et al. 2018). Unsupervised learning methods, like Zero-DCE, do not need paired images but encounter challenges in training stability and loss function convergence (Guo et al. 2020). Zero-shot learning strategies, which optimize using only a single low-light image, have strong generalization capabilities but suffer from insufficient information and reliance on prior knowledge, resulting in lower quantitative performance

(Li et al. 2022). Overall, existing methods still face challenges in reducing paired dataset dependence, improving model generalization, and ensuring training stability.

To overcome the aforementioned challenges, this paper proposes a low-cost, lightweight tunnel luminaire detection scheme based on Mask R-CNN, achieving high detection accuracy across multiple lighting sections. Addressing the brightness difference between tunnel luminaires and the background in dark environments, we propose an object brightness enhancement data augmentation method. Building on traditional algorithms, object brightness enhancement (OBE) selectively adjusts the pixels of the object, making the object features more prominent and easier for the model to learn. This scheme is more feasible and efficient in practical applications, providing a new effective approach for the safety management of tunnel lighting (Qin et al. 2025).

2. METHODS

2.1 Proposed Tunnel Luminaire Detection Scheme Overview

The model’s input data comprises a set of preprocessed and annotated gray-scale tunnel images. As shown in Figure 1, before training the model, the data must undergo object brightness enhancement. This is because increasing the difference in brightness between the tunnel luminaires and the background enables the Mask R-CNN to capture luminary features effectively. Therefore, we employed four methods to segment the pixels within the bounding box (bbox) into the foreground and background. In addition, we selectively enhanced the foreground’s brightness to improve the luminary contrast details.

Although our study only requires the bounding boxes of tunnel luminaires, Mask R - CNN has a more comprehensive feature extraction and processing pipeline and significant advantages in accuracy over object - detection - only networks like YOLO. In contrast, YOLO prioritizes speed in object detection, which may reduce its accuracy in complex scenarios.

During tunnel luminaire detection using the Mask R-CNN method, the first step involves preprocessing and inputting the images into the backbone network to extract features, such as edges and textures. Then, these features are used by the Region Proposal Network (RPN) to generate Regions of Interest (ROI). The ROIAlign layer pools the ROIs into fixed-sized feature maps for subsequent processing. As a result, the model achieves accurate luminaire detection and segmentation through N-class classifiers, bounding box regression, and mask generation steps (He et al. 2017).

To improve the small object detection performance, we used ResNet50-FPN as the backbone network, which enhances the recognition ability of small-sized objects like tunnel luminaires through multi-scale feature extraction. Furthermore, considering the limited number of samples in the object domain, we employed transfer learning techniques to initialize the weights using a pre-trained model on the COCO dataset (Lin et al. 2014), effectively avoiding overfitting issues and reducing the reliance on a large amount of training data.

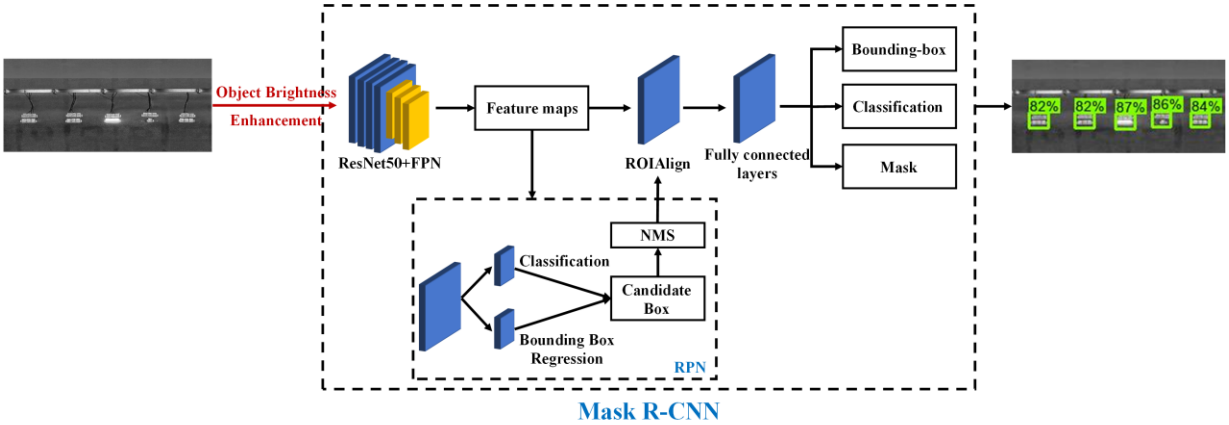

Figure 1. Overview of the proposed tunnel luminaire detection scheme (Framework excerpted from Figure X in Qin et al. 2025, redrawn in this paper)

2.2 Object Brightness Enhancement (OBE)

We observed that in tunnel image datasets, some luminaires (i.e., turned-on lights) exhibit significantly higher brightness than their surroundings, making these high-brightness lights easier to learn and detect in Figure 2. Therefore, to improve the detection accuracy of the Mask R-CNN model, we introduced the object brightness (OBE) method in addition to the standard data augmentation techniques. This enhancement method increases the brightness contrast between object areas and backgrounds, improving the model’s luminaire feature learning process.

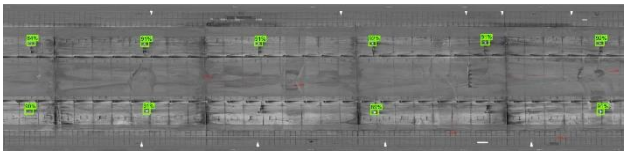

Figure 2. Detection superiority of turned-on lights over the turned-off ones.

We aim to highlight the luminaires within the bboxes while minimizing the overall impact on image contrast. Thus, in practice, pixels within the bbox region exceeding a specified threshold were selectively enhanced. Moreover, the brightness enhancement strategy was optimized using iterative adjustments to the threshold and enhancement magnitude based on training observations. These results were contrasted with scenarios where no brightness enhancement was applied to assess the

effectiveness of this approach. In addition, the enhancement range was set from 1.1 to 1.3 times the original brightness, balancing image quality and processing efficiency. To determine the threshold, we employed four distinct strategies to different image characteristics and application scenarios:

(1) Fixed Threshold Method
It sets a simple fixed threshold of 128 for gray-level value segmentation of the image.

(2) Gray-level Median Method
This method computes the gray-level histogram within the bbox and selects the median as the threshold to accommodate varying gray-level distribution characteristics across different regions.

(3) Kapur’s Entropy Method
This is an approach that utilizes the maximum entropy principle to determine an optimal threshold, ensuring maximal information retention after segmentation (Kapur et al. 1985).

(4) Otsu’s Method
This is an automatic and unsupervised method for computing the optimal image threshold, maximizing inter-class variance to achieve adaptive image binarization (Otsu 1979).

In the experimental section, we extensively compared the methods’ performances on tunnel image datasets to validate their effectiveness and applicability (Qin et al. 2025).

3. EXPERIMENTAL SETTINGS

3.1 Experimental Data

3.1.1 Image Collection: In this study, gray-scale images of a specific tunnel were obtained using the highway-tunnel fast detection system. This system is equipped with various sensors, cameras, and laser scanners to collect high-precision tunnel images, three-dimensional spatial information, and road data. The original images were preprocessed to simplify the image information, eliminate color interference, and highlight the tunnel’s internal structure and features. Additionally, as gray-scale images only contain brightness information, the significant differences in brightness between the luminaires and the surrounding environment facilitated more accurate positioning of the luminaires and provided clearer and more reliable features for the subsequent luminary detection algorithm.

3.1.2 Dataset Construction: As shown in Figure 3, the single image resolution collected in this study was 8143×1921, with each image corresponding to a 50m tunnel segment. A total of 18 images were gathered. To balance training efficiency and accuracy, the image size was reduced by a factor of five while retaining the mileage information. These processed images formed the foundational dataset for this experiment. In addition, labeling software was utilized to roughly annotate the luminaires. Then, the tunnel images were categorized into three classes based on various illumination levels: bright, dim, and darker. For each category, one image was randomly selected for training, two for the validation, and the remaining images constituted the test set with a ratio of 3:6:9. The training set contained 120 effectively annotated bbox samples, the validation set comprised 214 samples, and the test included 247 samples. Considering that the collected data output type was orthophoto images, various operations including affine transformation, image inversion, mirroring, Gaussian blur, and image brightness and contrast adjustments were employed to preserve the object position features and simulate different lighting conditions in the tunnel environment. This augmentation expanded the training set to 600 images. The final division and category statistics for the experimental data are presented in Table 1.

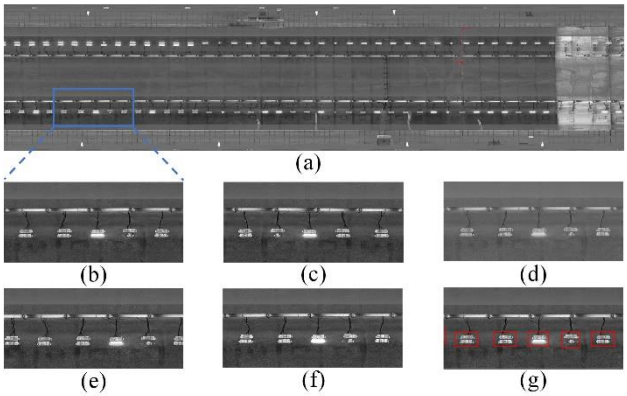

Figure 3. Data collection, augmentation, and annotation results; (a) An example tunnel image; (b) Detailed display of tunnel luminaires; (c) Mirroring; (d) Global brightness adjustment; (e) Affine transformation; (f) Enhanced object brightness; (g) Tunnel luminaire annotation results.

Dataset	Before Augmentation		After Augmentation	
	Number of images	Number of luminaires	Number of images	Number of luminaires
Training	3	120	600	24000
Validation	6	214	6(not augmented)	214
Test	9	247	9(not augmented)	247
Total	18	581	615	24461

Table 1. Experimental data set division (Data excerpted from Table 1 in Qin et al. 2025)

3.2 Experimental Environment and Parameters

The hardware environment for these experiments included a 12th Gen Intel Core i9-12900K 3.20 GHz processor and an NVIDIA RTX 4060Ti GPU with 8GB of memory. The software environment consisted of Windows 10, PyTorch 2.1 deep learning framework, CUDA 12.1, cuDNN 8.8.1, and Python 3.8. In terms of model training parameter settings, the stochastic gradient descent (SGD) algorithm was used as the optimizer for network model training, with a momentum of 0.9, an initial learning rate of 0.001, a batch size of 8, and 400 training epochs. For the pre-trained ResNet-50 weights from PyTorch, only the last three residual blocks were set to receive gradient updates, while the parameters of other layers remained unchanged, which helps in reducing training time and the risk of overfitting.

3.3 Other example

This study uses precision, recall, F1-score, average precision (AP) and mean average precision (mAP) as accuracy evaluation metrics.

Intersection over Union (IoU) is a measure of the overlap between the predicted bounding box and the actual bounding box, which significantly affects all evaluation metrics discussed in this article. By default, this article assumes an IoU threshold

of 0.5. The formula for calculating IoU is:

$$\text{IoU} = \frac{Area\ of\ Overlap}{Area\ of\ Union} \times 100\% \quad (1)$$

where the Area of Overlap is the region where the predicted box and the actual box intersect, and the Area of Union is the total area covered by both the predicted box and the actual box, excluding the overlapping region.

Precision reflects the proportion of correctly detected objects within the detected objects of that category. Recall reflects the proportion of correctly predicted objects among the actual objects of that category, and the F1-score is used to comprehensively evaluate both precision and recall. The calculation formulas are as follows:

$$\text{Precision}(P) = \frac{T_P}{T_P + F_P} \times 100\% \quad (2)$$

$$\text{Recall}(R) = \frac{T_P}{T_P + F_N} \times 100\% \quad (3)$$

$$\text{F1} - \text{score} = 2 \times \frac{P \times R}{P + R} \quad (4)$$

where T_P represents the number of correctly detected objects, F_P denotes the number of incorrectly detected objects, and F_N represents the number of missed correct objects.

In this study, since the detection only includes the category of tunnel lighting fixtures, AP and mAP are equivalent. Their calculation formulas are as follows, where classes represent the total number of categories in the detection task:

$$\text{mAP} = \frac{1}{\text{classes}} \sum_{i=1}^{\text{classes}} \int_0^1 P(R)\text{d}(R) \quad (5)$$

$$\text{AP} = \int_0^1 P(R)\text{d}(R) = \text{mAP} \quad (6)$$

Therefore, we choose to evaluate the model's performance at different levels of overlap by calculating AP at a specific IoU threshold：

(1) AP50

Refers to AP evaluated at an IoU threshold of 0.5. A prediction is considered accurate if the IoU between the predicted and ground-truth bounding boxes is ≥ 0.5. This metric evaluates the model's localization accuracy under a moderate overlap criterion.

(2) AP75

Denotes the AP at a stricter IoU threshold of 0.75. Here, predictions must achieve an IoU ≥ 0.75 with the ground truth to be deemed correct. This threshold assesses the model's precision in scenarios requiring a high degree of spatial alignment.

(3) AP50:95

Computed by averaging the APs obtained at ten IoU thresholds, ranging from 0.5 to 0.95 in 0.05 increments. This composite metric offers a robust evaluation of the model's performance across a wide range of IoU standards, serving as a benchmark for comparative analysis of object detection algorithms.

4. EXPERIMENTAL RESULTS AND ANALYSIS

To comprehensively evaluate the effectiveness of the OBE model in tunnel luminaire object detection, this study designed one control group and four experimental groups: (1) The control group used the Mask R-CNN model with standard data augmentation techniques; (2) Each experimental group applied a unique OBE method, with four distinct methods tested in total. Each experimental group was run on the same tunnel luminaire dataset and performance was compared using the established evaluation metrics. The experimental results reveal the advantages and disadvantages of single versus combined strategies in improving detection accuracy, robustness, and practicality, thus providing empirical evidence for the potential application of deep learning models in similar visual detection tasks.

4.1 Effectiveness Analysis of OBE

Table 2 compares the effects of four unique OBE methods on the test set. Each method was applied in a separate experimental group. The results show that all methods improved some metrics. Specifically, Kapur-1.1 achieved the best Recall, F1-score, AP50:95, and AP50. Additionally, Table 3 ranks the F1-score and AP50 within the brightness range (best = 1, worst = 3) and calculates the sum and mean to observe the overall performance of different brightness levels in all experimental groups. The results show that when the brightness level is 1.3, the average ranking is the lowest and the overall performance is the worst, proving that the increase in the target brightness level does not necessarily lead to better results.

Algorithm	Level	Precision	Recall	F1	AP50:95	AP50	AP75
None	0	0.906	0.779	0.837	0.196	0.625	0.062
Fixed	1.1	0.974	0.686	0.805	0.256	0.763	0.062
	1.2	0.955	0.779	0.858	0.210	0.740	0.038
	1.3	0.947	0.731	0.825	0.189	0.651	0.030
Median	1.1	0.944	0.683	0.792	0.224	0.716	0.043
	1.2	0.952	0.804	0.872	0.207	0.678	0.058
	1.3	0.959	0.786	0.864	0.202	0.718	0.031
Kapur	1.1	0.949	**0.823**	**0.881**	**0.234**	**0.776**	0.029
	1.2	0.950	0.779	0.856	0.189	0.674	0.030
	1.3	0.948	0.660	0.778	0.163	0.565	0.027
Otsu	1.1	0.948	0.737	0.829	0.232	0.747	**0.063**
	1.2	**0.983**	0.709	0.824	0.216	0.754	0.036
	1.3	0.971	0.680	0.800	0.194	0.686	0.035

Table 2. Performance comparison of OBE on Mask R-CNN (Data excerpted from Table 4 in Qin et al. 2025)

Level	Algorithm	F1	AP50	Mean
1.1	Fixed Median Kapur Otsu	3 3 1 1	1 2 1 2	1.75
1.2	Fixed Median Kapur Otsu	1 1 2 2	2 3 2 1	1.75
1.3	Fixed Median Kapur Otsu	2 2 3 3	3 1 2 3	**2.375**

Table 3. Ranking of F1-Score and AP50 for all experiments across brightness levels (Partial data excerpted from Table 7 in Qin et al. 2025)

The possible reasons why the enhancement of the target brightness level fails to bring better improvement effects are as follows: (1) Aggressive brightness enhancement leads to the model overfitting specific training data features (e.g., enhanced brightness differences) while ignoring other important ones. (2) If the model is trained only on data where brightness differences are significantly increased, it may not be adequately generalized to various brightness conditions encountered in actual applications.

4.2 Ablation Study of the New Detection Scheme

As shown in Table 2, using Kapur-1.1 yielded the highest detection accuracy. To evaluate the contribution of OBE in the new scheme, an ablation experiment was conducted, with the results presented in Table 4. By incorporating OBE, we significantly improved all metrics except for AP75. Notably, the F1-score and AP50 reached 0.881 and 0.776, respectively, representing improvements of 0.044 and 0.151 over the original result. Figure 4 intuitively shows the significant improvements of Kapur-1.1 on the detection effect of Mask R-CNN. Overall, this scheme delivered more accurate outcomes, thereby validating the effectiveness of our model improvement strategy.

Model	Precision	Recall	F1	AP50:95	AP50	AP75
Mask R-CNN	0.906	0.779	0.837	0.196	0.625	**0.062**
+OBE(Kapur-1.1)	**0.949**	**0.823**	**0.881**	**0.234**	**0.776**	0.029
Difference	0.043	0.044	0.044	0.038	0.151	-0.033

Table 4. Comparison of ablation experimental results

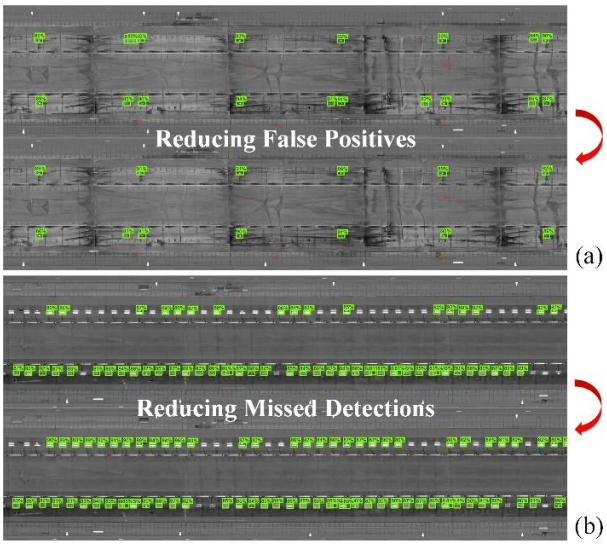

Figure 4. Improvement effects of OBE on Mask R-CNN; (a) Reducing False Positives; (b) Reducing Missed Detections.

5. CONCLUSIONS AND DISCUSSION

Given the complexities of tunnel environments, including numerous luminaires, low illumination, and the challenges involved in small-object detection, this study proposes a tunnel luminaire detection scheme based on Mask R-CNN. The research utilizes gray-scale tunnel images as the dataset, employing the Mask R-CNN framework enhanced by transfer learning with a ResNet-FPN feature fusion network to improve small luminary detection. Various strategies were employed to enhance the contrast in brightness between tunnel luminaires and the background, enabling Mask R-CNN to better learn the specific object features. The results demonstrated that the proposed method achieved a precision of 94.9%, a recall rate of 82.3%, an F1-score of 0.881 and an AP50 of 0.776 on the test set, improving these metrics by 4.3%, 4.4%, 0.044, and 0.151, respectively, compared to the original model. This scheme effectively improves the detection performance of tunnel luminaires, achieving accurate annotation and efficient positioning.

The primary conclusions of this study include:

(1) For the task of detecting tunnel luminaires under low illumination conditions and numerous small objects, the objective detection approach based on Mask R-CNN and transfer learning achieves excellent results.

(2) Using OBE improves the accuracy of Mask R-CNN without increasing its complexity. This approach allows for the prediction of extensive data from limited datasets, meeting engineering requirements.

We have also found that OBE, in the simple dark environment of a tunnel, can improve accuracy without the complexity of other low-light image enhancement methods. It does not require pre-training or computation of the entire image, thus reducing the cost of pre-processing.

While our approach has been specifically tailored for tunnel luminaire detection, the underlying principles and methodologies employed could potentially be adapted to other object detection tasks in similarly challenging environments:

The techniques used for brightness balancing may find utility in environments with suboptimal lighting conditions, such as underwater detection and cave mapping. In such situations, OBE could enhance the visibility of marine life or geological features, which are often subject to low light and varying clarity.

Building on these potential applications, future research could explore the following directions:

(1) Broader Environmental Applications: We aim to test and refine our model's adaptability to various challenging environments, leveraging OBE where appropriate. This will involve assessing the model's performance and making necessary adjustments to accommodate different lighting conditions, object densities, and environmental complexities.

(2) Expanding and diversifying the training dataset to include various tunnel environments and luminaire configurations, thereby enhancing the model’s generalizability and adaptability.

(3) Exploring the integration of other sensor data types, such as LIDAR point cloud data, with image data to provide more comprehensive environmental information, thereby improving detection accuracy and robustness.

By embracing these future directions, we anticipate that our research will not only advance the field of tunnel luminaire detection but also contribute to the broader application of intelligent object detection in diverse and challenging environments (Qin et al. 2025).

ACKNOWLEDGEMENTS

This work is supported by the Guangdong Province Key Research and Development Program Project (Grant No. 2022B0101070001), the National Key Research and Development Program Project (Grant No. 2023YFC3807500), the National Natural Science Foundation of China (Grant No. 42104012, 62201622, 42001407), the Shenzhen Science and Technology Program (Grant No. JCYJ20220531101812028, 20231120190100001, ZDSYS20210929115800001, 20231121094609001), and Key Laboratory Open Fund Project of Shenzhen Technology Institute of Urban Public Safety; in part by the Guangdong Basic and Applied Basic Research Foundation (2024A1515010777); and the Guangdong Science and Technology Strategic Innovation Fund (the Guangdong–Hong Kong-Macau Joint Laboratory Program) (Project No. 2020B1212030009).

REFERENCES

Alidoost, F., Hahn, M., Austen, G., 2023. DEVELOPMENT OF A MACHINE VISION SYSTEM FOR DAMAGE AND OBJECT DETECTION IN TUNNELS USING CONVOLUTIONAL NEURAL NETWORKS. *ISPRS Ann. Photogramm. Remote Sens. Spatial Inf. Sci*., X-1/W1-2023, 1-8. December.

Dai, L., Tang, C., Yang, G., Yang, H., Luo, J., Chen, Z., 2022. A Fault Detection Method and System for Highway Tunnel Dome Light Based on Improved YOLO with Localization Loss Function. *2022 4th International Conference on Industrial Artificial Intelligence (IAI)*, 1-6. August.

Guo, C., Li, C., Guo, J., Liu, W., 2020. Zero-Reference Deep Curve Estimation for Low-Light Image Enhancement. *Proceedings of the IEEE/CVF Conference on Computer Vision and Pattern Recognition (CVPR*), 185-194.

He, K., Gkioxari, G., Dollár, P., Girshick, R., 2017. Mask R-CNN. *2017 IEEE International Conference on Computer Vision (ICCV)*, 2980-2988.

Hou, Q., Tarko, A. P., Meng, X., 2018. Analyzing Crash Frequency in Freeway Tunnels: A Correlated Random Parameters Approach. *Accident Analysis & Prevention*, 111, 94-100. February.

Jobson, D. J., Rahman, Z., Woodell, G. A., 1997. A Multiscale Retinex for Bridging the Gap Between Color Images and the Human Observation of Scenes. *IEEE Transactions on Image Processing*, 6(7), 965-976.

Kapur, J., Sahoo, P., Wong, A., 1985. A New Method for Gray-Level Picture Thresholding Using the Entropy of the Histogram. *COMPUTER VISION GRAPHICS AND IMAGE PROCESSING*, 29(3), 273-285.

Li, C., Zhang, Y., Guo, J., Liu, Y., 2022. Low-Light Image and Video Enhancement Using Deep Learning: A Survey. *IEEE Transactions on Pattern Analysis and Machine Intelligence*, 44(12), 9396-9416.

Lin, T.-Y., et al., 2014. Microsoft COCO: Common Objects in Context. *2014 European Conference on Computer Vision (ECCV)*, Zurich, Switzerland, 740-755.

Lu, J., Dong, F., Hirota, K., 2015. Location Detection of Informative Bright Region in Tunnel Scenes Using Lighting and Traffic Lane Cues. *Journal of Advanced Computational Intelligence and Intelligent Informatics*, 19(2), 255-263. March.

Otsu, N., 1979. A Threshold Selection Method from Gray-Level Histograms. *IEEE Transactions on Systems, Man, and Cybernetics*, 9(1), 62-66.

Pizer, S. M., Amburn, E. P., Austin, J. D., Cromartie, R., Geselowitz, A., Greer, T., Holloway Jr, J. R., Perry, P. D., Strelow, D., 1987. Adaptive Histogram Equalization and Its Variations. *Computer Vision, Graphics, and Image Processing*, 39(3), 355-368.

Puente, I., González-Jorge, H., Martínez-Sánchez, J., Arias, P., 2014. Automatic Detection of Road Tunnel Luminaires Using a Mobile LiDAR System. *Measurement*, 47, 569-575. January.

Qin, X., Xu, B., Wang, C., Liu, L., Xie, L., Liu, R., Hu, M., Chen, X., 2025. Enhanced Mask R-CNN for luminaire detection through brightness balancing and distribution-guided optimization in tunnels. International Journal of Digital Earth, 18(1).

Wei, C., Wang, W., Yang, W., Liu, J., 2018. Deep Retinex Decomposition for Low-Light Enhancement. *ArXiv*, abs/1808.04560.

Xin, L., Shi, Z., Chen, Y., 2021. Robust Detection of Lighting LEDs by Analyzing the Geometric Structure of the Tunnel Interior Environment in Vehicle-Mounted Video Sequences. *2021 40th Chinese Control Conference (CCC)*, 3327-3333. July.

Yang, R., Pan, Z., Jia, X., Zhang, L., Deng, Y., 2021. A Novel CNN-Based Detector for Ship Detection Based on Rotatable Bounding Box in SAR Images. *IEEE Journal of Selected Topics*

in Applied Earth Observations and Remote Sensing, 14, 1938-1958.

Yang, W., Li, Z., Liu, Q., Zhang, H., Zhang, L., 2020. Advancing Image Understanding in Poor Visibility Environments: A Collective Benchmark Study. *IEEE Transactions on Image Processing*, 29, 5737-5752.